

VTT Technical Research Centre of Finland

Oxidative modification of cellulosic fibres by lytic polysaccharide monooxygenase AA9A from *Trichoderma reesei*

Marjamaa, Kaisa; Rahikainen, Jenni; Karjalainen, Marika; Maiorova, Natalia; Holopainen-mantila, Ulla; Molinier, Matthieu; Aro, Nina; Nygren, Heli; Mikkelsen, Atte; Koivula, Anu; Kruus, Kristiina

Published in:
Cellulose

DOI:
[10.1007/s10570-022-04648-w](https://doi.org/10.1007/s10570-022-04648-w)

E-pub ahead of print: 04/06/2022

Document Version
Publisher's final version

License
CC BY

[Link to publication](#)

Please cite the original version:

Marjamaa, K., Rahikainen, J., Karjalainen, M., Maiorova, N., Holopainen-mantila, U., Molinier, M., Aro, N., Nygren, H., Mikkelsen, A., Koivula, A., & Kruus, K. (2022). Oxidative modification of cellulosic fibres by lytic polysaccharide monooxygenase AA9A from *Trichoderma reesei*. *Cellulose*. <https://doi.org/10.1007/s10570-022-04648-w>



VTT
<http://www.vtt.fi>
P.O. box 1000FI-02044 VTT
Finland

By using VTT's Research Information Portal you are bound by the following Terms & Conditions.

I have read and I understand the following statement:

This document is protected by copyright and other intellectual property rights, and duplication or sale of all or part of any of this document is not permitted, except duplication for research use or educational purposes in electronic or print form. You must obtain permission for any other use. Electronic or print copies may not be offered for sale.



Oxidative modification of cellulosic fibres by lytic polysaccharide monooxygenase AA9A from *Trichoderma reesei*

Kaisa Marjamaa · Jenni Rahikainen · Marika Karjalainen · Natalia Maiorova · Ulla Holopainen-Mantila · Matthieu Molinier · Nina Aro · Heli Nygren · Atte Mikkelsen · Anu Koivula · Kristiina Kruus

Received: 12 January 2022 / Accepted: 13 May 2022
© The Author(s) 2022

Abstract Lytic polysaccharide monooxygenases (EC1.14.99.53-56, LPMOs) are oxidative enzymes with the capability to enhance lignocellulose saccharification as well as nanofibrillation of cellulosic fibres. The parameters affecting the efficiency of oxidative modification of cotton linters and softwood kraft fibres by LPMO from *Trichoderma reesei* (*Tr* AA9A) were studied here. Circular dichroism experiments were carried out to analyze the thermal stability and to indicate the optimum temperature for the experiments. The enzyme was found to be most thermostable at pH 5 but can tolerate up to 40–50 °C at

neutral pH. The enzymatic fibre oxidation efficiency was found to be dependent on reductant (gallic acid) and hydrogen peroxide supply in a pH dependent manner. A high resolution UHPLC-IM-MS method was used for identification of oxidized oligosaccharides released in the enzymatic treatments. A microscopy method was applied for analysis of single fibre dissolution kinetics of *Tr* AA9A pretreated softwood kraft fibres, demonstrating that the oxidative enzymatic treatment facilitated the fibre dissolution and degraded the fibre surface structures, which prevent swelling.

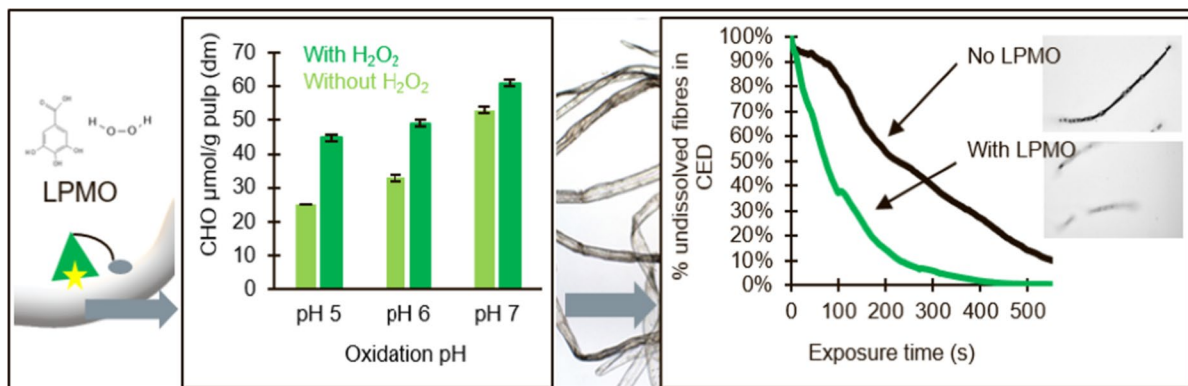
Supplementary Information The online version contains supplementary material available at <https://doi.org/10.1007/s10570-022-04648-w>.

K. Marjamaa (✉) · J. Rahikainen · M. Karjalainen · N. Maiorova · U. Holopainen-Mantila · M. Molinier · N. Aro · H. Nygren · A. Mikkelsen · A. Koivula · K. Kruus
VTT Technical Research Centre of Finland Ltd,
P.O.Box 1000, 02044 VTT Espoo, Finland
e-mail: kaisa.marjamaa@vtt.fi

Present Address:

K. Kruus
Department of Bioproducts and Biosystems, School
of Chemical Technology, Aalto University, P.O.
Box 16300, 00076 Espoo, Finland

Graphical Abstract



Keywords Lytic polysaccharide monooxygenase · LPMO · Cotton · Softwood · Fibre · *Trichoderma reesei* · Gallic acid · Hydrogen peroxide · CED · Dissolution · Oxidation · UHPLC-IM-MS · TTC

Introduction

Oxidation is used in improvement of cellulose and cellulosic fibre properties in a range of applications areas, from medical and cosmetics to papermaking, composites, textiles and cellulose derivatives (reviewed in Coseri et al. 2013). At a molecular level, oxidation introduces new carboxyl or carbonyl groups to the cellulose polymer and can cause cleavages of the glycosidic linkages (Potthast et al. 2006). These molecular level modifications can alter technical cellulose or fibre properties, such as charge, viscosity, fibre strength and binding properties (Potthast et al. 2007).

Chemical oxidation of cellulose can be carried out using non-selective oxidants, such as ozone (Johansson and Lind 2005), or selective oxidants, such as periodates or nitroxyl radicals [e.g. 2,2,6,6-Tetramethyl-1-piperidinyloxy (TEMPO)] (Potthast et al. 2007; Isogai et al. 2011; Patel et al. 2011). Biocatalytic oxidation methods provide interesting options due to the low energy input, selectivity and environmental safety of the enzymatic catalysis. In addition, chemo-enzymatic oxidation of cellulose can be achieved with polyphenol oxidases (laccases) or peroxidases in combination

with a suitable mediator compound. In such systems, the enzyme oxidizes the mediator, such as TEMPO, which in turn oxidizes the cellulose molecule (Quintana et al. 2017).

Lytic polysaccharide monooxygenases (EC1.14.99.53-56, LPMOs) are a class of enzymes found in fungi, bacteria, viruses, insects and plants, and characterized by an ability to directly oxidize polysaccharides, including cellulose, starch, chitin and/or hemicelluloses (see also <http://www.cazy.org/Auxiliary-Activities.html>) (Vaaje-Kolstad et al. 2010; Hemsworth et al. 2015; Lo Leggio et al. 2015; Hüttner et al. 2019; Vandhana et al. 2022). The known cellulose oxidizing LPMOs are regioselective and can hydroxylate at C1 and/or dehydrogenate at C4 position of anhydroglucose units in cellulose, leading to a cleavage of the glycosidic linkage and formation of new end-groups on the cellulose polymer, either δ -1,5 lactones or 4-ketoaldoses (Hemsworth et al. 2015; Quinlan et al. 2011). Characterization of LPMO activity is demanding and has been mainly carried out by analysing the soluble products released from the insoluble polysaccharide substrates.

Three-dimensional structures of several LPMOs have been solved, demonstrating that despite of the low sequence similarities, LPMOs share a similar Ig-like β -sandwich folds with a flat substrate binding surface containing a single copper ion, which is essential for the oxidative reactions (Quinlan et al. 2011). The LPMO activity requires also presence of a suitable electron donor, which reduces the Cu(II) in the active site to Cu(I). LPMOs have been reported

to accept various types of reductants, including e.g. monoaromatics, dehydrogenase enzymes, and pigments (Langston et al. 2011; Cannella et al. 2016). Molecular oxygen was initially thought to be the co-substrate of LPMOs in the polysaccharide oxidation and the reaction scheme involved stoichiometric consumption of the reductant as a source of electrons (Vaaje-Kolstad et al. 2010; Phillips et al. 2011; Frandsen et al. 2016; Meier et al. 2018). Recent observations have shown that at least for some LPMOs, the activity can be substantially increased by supplementing the reaction with hydrogen peroxide (H_2O_2). This has led to a suggestion of a reaction scheme, in which H_2O_2 acts as a co-substrate for LPMOs and a reductant is needed only for the so called priming reduction of the active site copper (Bissaro et al. 2017; Kuusk et al. 2019).

Concerning different applications, LPMO enzymes have been mostly studied in the area of lignocellulose saccharification for production of second generation biofuels. In this application, they have been reported to remarkably enhance the efficiency of lignocellulolytic enzyme cocktails (Müller et al. 2015; Rodríguez-Zúñiga et al. 2015). In material applications, some LPMOs have been successfully applied in enhancing nanofibrillation of cellulosic fibres (Villares et al. 2017; Hu et al. 2018; Moreau et al. 2019; Valls et al. 2019). Interestingly, in these studies, only low amount of sugar release, and subtle change in fibre structure were typically associated to the enhancement of the fibrillation by the LPMO enzymes.

The LPMO AA9A from *Trichoderma reesei*, a mesophilic filamentous fungus and a common industrial enzyme production host, was initially characterized as a low activity endoglucanase IV (or Cel61A) (Saloheimo et al. 1997; Karlsson et al. 2001). The cellulose oxidizing activity of the *Tr* AA9A leading to soluble C1 and C4 oxidation products was demonstrated a few years ago (Tanghe et al. 2015; Pierce et al. 2017; Song et al. 2018). The *Tr* AA9A enzyme consists of a catalytic module linked to a carbohydrate-binding module (CBM1), which enhances its binding to cellulose (Saloheimo et al. 1997; Hansson et al. 2017). The enzyme has been recently reported to oxidize cellulose in presence of molecular oxygen and/or H_2O_2 (Kont et al. 2019, 2020; Jones et al. 2020).

Cellulosic fibre dissolution and cellulose derivatisation are typically carried out via chemical means, but can cause an excess chemical consumption and toxic waste formation (Li et al. 2018). It has been shown that the fibre reactivity can be improved by pretreating fibres with an endoglucanase-type of cellulase, thus leading to lower chemical consumption and more sustainable processes (Rahkamo et al. 1998; Ibarra et al. 2010; Grönqvist et al. 2014; Rahikainen et al. 2019). Recently, we showed that similar effect can be achieved on softwood kraft fibres by oxidation with an LPMO (Ceccherini et al. 2021). However, typical changed molar mass (Mw) and porosity values, connected with faster dissolution rates of endoglucanase treated fibres, were not detected by the *Tr* AA9A treatment, suggesting that the basis of the improved reactivity can be different from that of the endoglucanase. In addition, based on the known complexity of the LPMO catalyzed reactions, better insight into the parameters affecting the efficiency of *Tr* AA9A catalyzed oxidation of fibres is needed.

In the present study, a systematic assessment of LPMO-assisted treatments of cotton and softwood fibres was carried out to elucidate the factors, which affect the *Tr* AA9A stability and efficiency in oxidative fibre modification. A spectrophotometric aldehyde measurement was used as a fast method to follow accumulation of oxidation products in cellulosic fibres. Furthermore, a ultra high-performance chromatography (UHPLC) combined to ion mobility (IM) and mass spectrometry (MS) detection was used for simultaneous identification of oxidized soluble oligosaccharides resulting from enzymatic oxidation. Finally, a microscopy-based method was used for exploring single-fibre dissolution kinetics and changes in the morphology of the fibres in cupriethylenediamine (CED), in order to better understand the reasons for the better solubility of the LPMO treated fibres.

Materials and methods

Enzymes and cellulosic substrates

The *Tr* AA9A LPMO and *Tr* Cel45A endoglucanase were produced and purified as described in Kont et al.

(2019) and Ceccherini et al. (2021). Soluble protein concentrations (mg/mL) in the enzyme preparations were analyzed using Biorad DC kit and BSA standards according to the manufacturer's instructions (BioRad, Hercules, California, USA). Whatman No1, prepared from cotton linters, was purchased from Sigma Aldrich and bleached softwood kraft pulp was received as dry sheets from Metsä Fibre Rauma mill. The sheets were disintegrated to separate fibres and the wetted pulps was washed to sodium form prior use.

Wet disintegration of Whatman No 1 was slightly modified from the SCAN 18:65 method: filter paper (60 g) was torn into pieces and soaked for 4 h in ultrapure water in final volume of 2.5 L. The wet pulp was homogenized in a pulp disintegrator (Lorentzen & Wettre, Stockholm, Sweden) for 30 000 revolutions at room temperature. Solids were collected by filtration through a 60 µm sieve (Medifab 03-60/42, Sefar, Heiden, Switzerland) in a Büchner-funnel, and the pulp was further homogenized with a kitchen mixer (Kenwood Ltd, Havant, UK). The homogenized fibres were diluted into a final volume of 5 L with reverse osmosis (RO) purified water and HCl was added to a final concentration of 0.01 M. The slurry was allowed to stand at room temperature for 15 min with occasional mixing. The fibres were washed twice with 5 L of RO water (incubation for 15 min followed by filtration) and diluted into final volume of 5 L with RO water. Sodium bicarbonate was added to a final concentration of 5 mM and pH was adjusted to 8.5 with 1 M NaOH. The slurry was incubated at room temperature for 15 min with occasional mixing followed by washing with ultrapure water five times as described earlier. The wet cotton linter pulp was stored in cold (4 °C) prior to use. The softwood pulp was treated in a similar manner as the filter paper. The shredded sheets were allowed to wet overnight in RO-water and cold disintegration was carried out using the Lorentzen & Wettre pulp disintegrator (50 g dry pulp/2 L RO-water, 30000 rpm) as washed to sodium form as described above.

Circular dichroism of the *Tr* AA9A LPMO protein

Overall fold and thermal stability of the purified *Tr* AA9A was studied using circular dichroism (CD) spectroscopy. The buffers used in the experiments were 10 mM sodium acetate buffer pH 5 and

25 mM sodium phosphate buffers pH 6, 7 and 8. The enzyme concentration was 4.8 µM. The sodium acetate buffer was used in lower concentration than sodium phosphate buffer in order to minimise interference by UV adsorption of the carbonyl groups in the acetate buffer. The measurements were carried out using Chirascan CD spectrometer (Applied Photophysics, Leatherhead, Surrey, UK) equipped with a CD250™ cell holder (Quantum Northwest, Washington, USA). The temperature was controlled with a TC125 Peltier type controller (Quantum Northwest). The spectra were recorded twice in a 1 mm path length cuvette using a bandwidth of 1 nm and scanning from 240 to 190 nm with 0.5 nm interval and 2 s per each measurement point. Temperature induced unfolding was monitored at 202 nm using a temperature ramp program from 25 to 90 °C (rate 2 °C/min).

Oxidation of cotton linters with *Tr* AA9A

The cotton linters was treated at 1% (w/v) consistency with 5 to 20 mg of *Tr* AA9A/g of substrate in 50 mM sodium acetate buffer pH 5; 50 mM MES buffer pH 6; 50 mM MOPS buffer pH 7 and 50 mM Tris–HCl buffer pH 8 and with 1 mM of gallic acid (GA) as a reductant. The reactions were carried out in 2 mL Eppendorf tubes and 10 mg dry matter (dm) of cotton linters was treated in one reaction. All the reactions were carried out in triplicates. Treatments were carried out also in presence 0.2 or 0.7 mM H₂O₂. Control reactions were conducted with identical setups, but without either *Tr* AA9A or GA, or without either. The reactions were carried out at 45 °C in a shaker (800 rpm) with 6 h incubation time. After the incubation, liquid fractions were separated from solids by centrifugation (4 °C, 20187×g, 10 min) (5430R Eppendorf, Hamburg, Germany) and the solids were washed twice with MilliQ water. The liquids were frozen (– 20 °C) and the solids were lyophilized (Christ Alpha 2–4, B. Braun Biotech International, Melsungen, Germany) for 12 h.

Oxidation of softwood kraft fibres with *Tr* AA9A

The softwood fibres were treated at 3% (w/w) consistency with 0.25–5 mg of *Tr* AA9A/g substrate (dm) in either 50 mM sodium acetate buffer pH 5 or

50 mM sodium phosphate buffer pH 6 or 7 at 45 °C for 2–24 h. The reactions were carried out in shake flasks using 1 g of pulp and 1 mM GA as reductant. Some reactions were also carried out in presence of H₂O₂. The reaction time in these experiments was 6 h and the H₂O₂ was added gradually, with 0.2 mM addition in the beginning and after 2 and 4 h. A reference sample was prepared by treating the fibres with an endoglucanase *Tr Cel45A* at pH 7, 45 °C for 24 h. After the incubation, the liquids were separated by filtration, the liquid circulated one through the solids and finally the solids were washed 10 times with 10 mL of reverse osmosis water. Dry matter content of the washed samples was measured gravimetrically after oven drying (ca 0.8–1 g wet samples dried at 105 °C overnight). The wet samples were stored at 4 °C before further analyses.

UHPLC-IM-MS analysis of the soluble sugars

Analysis was performed on an Acquity UHPLC system, Waters (Milford, Massachusetts, USA) and Waters Synapt G2-S MS system Waters (Milford, Massachusetts, USA). Chromatography was performed using an HYPERCARB column, 3.0 µm 2.1×150 mm (Thermo Scientific, Massachusetts, Waltham, USA), kept at 65 °C. The runs were carried out at a flow rate of 0.4 mL/min with mobile phase A (10 mM ammonium acetate in water, pH 8) and B (acetonitrile). The gradient elution started at 100% A and maintained at 100% A for 1.0 min, then decreased to 72.5% A within 15 min and to 60% A within further 5.0 min, then directly returned to initial percentage and maintained for 10 min. Injection volume was 2 µL. Due to form of (M+Na)⁺ adducts, a post-column addition of NaCl (5 µg/mL) was performed, at flow rate of 5 µL/min.

Mass spectrometry was carried out using electrospray ionization (ESI) in a positive polarity mode. The capillary voltage was 2.8 kV, cone voltage 40 kV, source temperature 150 °C and desolvation temperature 500 °C. The cone and desolvation gas flow were set at 50 L/h (nitrogen) and 1000 L/h (nitrogen), respectively. Mass range was 100–1000 m/z. For analysis of native and oxidized species of cellooligosaccharides Ion mobility (IM) was used. Ion mobility was performed in a traveling-wave ion mobility (TWIM) cell. The gas flows were held at 180 mL/min He in the helium cell and at 90 mL/min nitrogen

in the Ion Mobility Separation cell. The IM traveling wave height was 40 V and its wave velocity was 450 m/s. For data acquisition was used MassLynx software (V4.1) and IM data processing was carried out by DriftScope software.

Relative quantitation of C1 and C4 oxidized products were based on the calibration curves of corresponding non-oxidized cello-oligosaccharides (cellobiose, celotriose and celotetraose). Standard solutions (0.05–100 µg/mL) of the non-oxidized cello-oligosaccharides were prepared in water. The calibration curves were determined by linear polynomial style without weighting and they showed correlation coefficients (r^2) higher than 0.99 in all cases.

Quantification of aldehydes in the fibre samples

The aldehydes in the insoluble cotton linter samples were quantified using a modified TTC (2,3,5-triphenyltetrazolium chloride) assay adapted from Obolenskaya et al (1991). This miniaturized spectroscopic method allowed carrying out assays in 2 mL tubes. The lyophilized cotton linter samples (10 mg) were homogenized in 500 µL of 0.2 M KOH by vortexing after which 500 µL of 0.2% (w/v) TTC reagent (Merck, Germany) was added. Tubes were mixed thoroughly by vortexing, heated for 10 min at 98 °C (Stuart block heater SBH 130D, Bibby Scientific, UK) and centrifuged at 20817×g for 5 min at 4 °C (5430R, Eppendorf, Germany). 500 µL of the supernatant was removed and 1500 µL of ice-cold 95% ethanol was added. Tubes were again mixed well by vortexing and centrifuged as previously. Absorbance at 546 nm of the supernatant was measured and concentrations of aldehydes were calculated according to the absorbances of the glucose standards with final concentrations of 8.6–137 µM. The micromolar amounts of aldehydes detected in the reaction volume was divided with the weight of the used pulp /reaction, resulting in aldehyde (CHO) values µmol/g of pulp (dm). Average and standard deviation of at least triplicate experiments was used to present the results.

The aldehyde groups in the softwood fibres were analysed with the TTC method according the published method (Obolenskaya et al 1991) described in detail in Ceccherini et al. (2021). The pulp samples (20 mg dm) were thoroughly mixed with 0.5 mL of 0.2 M KOH and 0.5 mL 0.2% aqueous solution of TTC was added. The samples were heated 3–10 min

in a boiling water bath and quickly cooled down in cold water. The soluble fraction was separated by filtration through glass filter and the pulp was washed several times with a small amount of ethanol until the pulp appeared colorless again and the total volume of filtrate was 10 mL. The aldehydes were quantified by measuring absorbance of the filtrates at 546 nm and using glucose as standard.

Size-exclusion chromatography

The fibre samples were dissolved in dimethylacetamide (DMAc)/8% LiCl using a solvent exchange method described in Berthold et al. (2001). The dissolution protocol began by activation with water, solvent exchange via methanol and DMAc, followed by ethyl isocyanate derivatisation assisted dissolution into DMAc/8% LiCl. Two to three replicates of each sample were dissolved. For analysis, the samples were diluted with DMAc providing final LiCl concentration of 0.8% and filtered (filter pore size 0.45 μm) before the measurement. The size exclusion chromatography (SEC) analysis was done using 2 \times PL gel MiniMixed A columns (Agilent, Santa Clara, California, USA) with a precolumn in DMAc/0.8% LiCl eluent (0.36 mL/min, T=80 °C) and the elution curves were detected using Waters 2414 refractive index detector (Waters, Milford, Massachusetts, USA). The molar mass distributions (MMD) were calculated against 8 \times pullulan (6100–708,000 g/mol) standards, using Waters Empower 3 software.

Microscopy technique for analysis of fibre dissolution

Dissolution of the softwood kraft fibres to alkaline cellulose solvent cupriethylenediamine (CED) were studied using a method modified from Mäkelä et al. (2018) and Rahikainen et al. (2019). Microscopy was done using a Zeiss AxioImager M.2 microscope (Carl Zeiss GmbH, Göttingen, Germany) with 2.5 \times objective (Zeiss EC Plan-Neofluar, numerical aperture of 0.085, Zeiss) and polarizer in the angle of 75°. The images were captured with a Zeiss AxioCam 506 CCD colour camera (Zeiss) in black and white mode and the Zen imaging software (Zeiss). The fibres were dispersed in water and 44–51 fibres were used from each sample for dissolution experiments. In one experiment, 2–3 fibres were placed on a microscopy slide under a cover slip. After this, a drop of 0.2 M CED (Oy FF-Chemicals

Ab, Haukipudas, Finland), dissolved in Milli-Q water, was added and allowed to reach the fibres by capillary forces. Microscopy images were captured every 1.0 s until the fibres were visibly disappeared.

The dissolution videos representing 14–48 individual fibres of each sample were analysed using automatic image and video processing methods. The 2D/projectional area of the fibres was analysed for all images in the video after wetting with CED, using a custom program developed in Matlab. The program outputs numerical tables recording the area of each fibre for every image (from which fibre dissolution rates were calculated), and dissolution curves (fibre area versus time), which allows to determine how the different treatments affected the fibre dissolution mechanism. Details of the video processing chain are given in Rahikainen et al. (2019). The method automatically extracts the moment in the video when the microscopy slides were uniformly wetted with CED. Then individual fibres are detected in every images using a maximum entropy threshold (Kapur et al. 1985) and tracked (i.e. matched with the corresponding fibre in the previous image) using a spatio-temporal consistency criterion inspired from (Molinier et al. 2005), while filtering out other objects (occasional non-fibrous material, air bubbles and other artefacts). The processing chain was slightly modified compared to Rahikainen et al. (2019), to account for specific challenges of the videos analysed in this study. Higher illumination changes and faint but uniformly spread artefacts (due to the fibre dissolution process) affected the detection of undissolved fibres. This was solved by controlling the sensitivity of the binarization process in the fibre detection stage, and adding buffers around fibres to avoid artefacts from being merged into real fibres.

Results and discussion

pH dependency of thermal stability of purified *Tr* AA9A protein

Enzyme stability and consequently functionality is dependent on prevailing temperature, solvent pH and buffer composition. Thermal stability of the *Tr* AA9A was studied at pH 5–8 with CD spectroscopy in 10 mM sodium acetate (pH 5) and 25 mM sodium phosphate (pH 6–8) buffers (Supporting information (SI) Fig. 1). The *Tr* AA9A was most stable in 10 mM

sodium acetate buffer at pH 5, in which the thermal midpoint of unfolding (T_m) of the enzyme was 64 °C. The temperature stability of *Tr* AA9A was impaired in the sodium phosphate buffers at higher pHs and ca 10 °C lower unfolding temperature was measured at pH 8 ($T_m = 51$ °C). At pH 6 and 7 the T_m values were 62 °C and 57 °C, respectively. The relation between pH and T_m of the *Tr* AA9A was similar to that of the major *T. reesei* cellobiohydrolase Cel7A (Boer and Koivula 2003). However, the *Tr* AA9A exhibited better stability at elevated pH than the *Tr* Cel7A: at pH 8, the T_m of *Tr* Cel7A was below 40 °C, while the T_m of *Tr* AA9A was still ca 50 °C. Singh et al. (2019) analyzed thermal stability of AA9 LPMO from thermophilic fungus *Thermoascus aurantiacus* in citrate, phosphate and Tris buffers in pH range 4–9, using intrinsic protein fluorescence and CD. In 20 mM MOPS buffer pH 7, the CD analysis showed a T_m of 69 °C for the *Ta* LPMO9A, suggesting that this LPMO had better stability at neutral pH compared to *Tr* AA9A (Singh et al. 2019). However, similar to the *Tr* AA9A, the *Ta* LPMO9A exhibited highest thermal stability at pH 5. At higher pHs, use of Trizma buffer as solvent was found to promote the stability of *Ta* AA9A (Singh et al. 2019). Calderaro et al. (2020) in turn used a thermal shift assay kit for assessing stability of LPMO9B from *Thielavia australiensis* in sodium acetate, BisTris/HCl and Tris/HCl buffers with pHs ranging from 3 to 8. Highest T_m (76 °C) was measured in sodium acetate buffer pH 5. Based on the CD analysis in the current work, the temperature selected for the LPMO-assisted fibre treatments at pH 5–8 was 45 °C.

Oxidation of cotton linters by *Tr* AA9A as a function of pH, H_2O_2 and enzyme load

Effect of reaction pH and H_2O_2 supply on oxidation of cotton linters by *Tr* AA9A was studied as a function of enzyme load in order to identify the parameters that affect the oxidation efficiency. According to the previous publications the *Tr* AA9A produces both C1 and C4 oxidation product when incubated with cellulose (Tanghe et al. 2015; Pierce et al. 2017; Hansson et al. 2017; Song et al. 2018). This was also detected here (Table 1, see also below). According to the relative quantitation of the released oligosaccharides using native oligosaccharides as standards, the carbonyl groups ($-C=O$) dominate among the *Tr* AA9A

oxidation products, suggesting that dehydrogenation at a C4 position of the glucose ring was the prevailing in oxidation of the cotton fibres. The LPMO catalyzed dehydrogenation at C4 position results in cellulose chain cleavage, with two new chain ends having a 4-ketoaldoses at the new non-reducing end and an aldehyde at the new reducing end, respectively. Consequently, the increasing amount of aldehydes in the insoluble substrate fraction (fibres) can be used to monitor the C4 oxidative cleavages by *Tr* AA9A. The aldehydes in the fibres were quantified using the spectrophotometric TTC assay, which was miniaturized to 2 mL scale in order to facilitate the analysis.

The reactions were carried out for 6 h at 45 °C in a pH range 5–8, with GA only, or in presence of 0.2 or 0.7 mM added H_2O_2 , and using 5–20 mg *Tr* AA9A/g substrate (dm) (Fig. 1). Reference reactions were carried out for each *Tr* AA9A dosage without the GA, in order to monitor aldehydes possibly arising from bound protein or any hydrolase impurities in the purified *Tr* AA9A sample.

The amount of aldehydes formed in the enzyme treatment at pH 5 and pH 6 was dependent on an enzyme load and addition of H_2O_2 (Fig. 1a, b). Highest amount of aldehydes [ca 12 $\mu\text{mol/g}$ pulp (dm)] was detected with the highest enzyme load (20 mg/g pulp) and when H_2O_2 was added to the reaction. At pH 5, concentration of H_2O_2 (0.2 or 0.7 mM) did not essentially affect the aldehyde amount, while at pH 6, the lower 0.2 mM H_2O_2 concentration produced higher amount of aldehydes. The reaction efficiency, in terms of aldehyde accumulation in fibres, within the given time frame (6 h) was thus dependent on enzyme load and H_2O_2 supply. At pH 5, a small but clear increase in the aldehyde content was seen also when the cotton linters were treated with *Tr* AA9A without GA, in particular when highest dosages [15–20 mg/g pulp (dm)] was used (Fig. 1a). This could be caused by some minor endoglucanase impurity in the *Tr* AA9A preparation, since the cellulases of *T. reesei* are commonly most active at acidic pH.

The effect of enzyme load and addition of H_2O_2 on the fibre oxidation level was remarkably different at pH 7 compared to the lower pHs (pH 5 and pH 6) (Fig. 1c). The highest amount of aldehydes [ca 14 $\mu\text{mol/g}$ pulp (dm)] was achieved already with the lowest protein load [5 mg/g pulp (dm)] and addition of H_2O_2 had no positive effect on aldehyde levels, suggesting that the catalytic efficiency of the

Table 1 Soluble sugars (mg/L) formed in 6 h treatment of cotton linters with *Tr*-AA9A [10 mg/g substrate (dm)] at pH 6 and pH 7, 45 °C, analyzed with UHPLC-IM-MS

Reaction	Glc	Glc2	Glc2-AldA	Glc2-diolC4	Glc3	Glc3-AldA	Glc3-diolC4	Glc3-KetoneC4	Glc4	Glc4-diolC4	Glc4-KetoneC4
pH 6											
GA + H ₂ O ₂	≤0.2	≤0.2	≤0.2	≤0.2	≤0.1	≤0.1	≤0.1	≤0.1	≤1.6	≤1.6	≤1.6
<i>Tr</i> -AA9A	≤0.2	≤0.2	≤0.2	≤0.2	≤0.1	≤0.1	≤0.1	≤0.1	≤1.6	≤1.6	≤1.6
<i>Tr</i> -AA9+GA	≤0.2	≤0.2	≤0.2	0.3±0.3	≤0.1	≤0.1	≤0.1	≤0.1	≤1.6	≤1.6	≤1.6
<i>Tr</i> -AA9A+H ₂ O ₂	≤0.2	≤0.2	≤0.2	0.2±0.02	≤0.1	≤0.1	≤0.1	≤0.1	≤1.6	≤1.6	≤1.6
<i>Tr</i> -AA9A+GA+H ₂ O ₂	0.2±0.2	0.8±0.0	0.6±0.0	4.7±0.2	1.7±0.1	0.2±0.1	1.2±0.0	0.5±0.1	3.0±0.3	1.5±0.7	≤1.6
pH 7											
GA + H ₂ O ₂	≤0.2	≤0.2	≤0.2	≤0.2	≤0.1	≤0.1	≤0.1	≤0.1	≤1.6	≤1.6	≤1.6
<i>Tr</i> -AA9A	≤0.2	≤0.2	≤0.2	≤0.2	≤0.1	≤0.1	≤0.1	≤0.1	≤1.6	≤1.6	≤1.6
<i>Tr</i> -AA9+GA	0.7±0.1	1.6±0.0	0.5±0.01	7.0±0.08	4.0±0.4	0.2±0.03	4.0±0.1	1.9±0.1	8.2±0.2	7.8±1.3	6.3±0.1
<i>Tr</i> -AA9A+H ₂ O ₂	≤0.2	≤0.2	≤0.2	≤0.2	≤0.1	≤0.1	≤0.1	≤0.1	≤1.6	≤1.6	≤1.6
<i>Tr</i> -AA9A+GA+H ₂ O ₂	1.2±0.0	2.2±0.2	0.7±0.01	10.1±0.9	5.8±0.4	0.3±0.00	5.3±0.2	2.6±0.1	12.1±1.0	11.7±1.8	7.9±0.7

Reactions were carried out with enzyme only (*Tr*-AA9A), enzyme and gallic acid (*Tr*-AA9A+GA), enzyme and H₂O₂ (*Tr*-AA9A+H₂O₂), or enzyme and both hydrogen peroxide and gallic acid (*Tr*-AA9A+GA+H₂O₂). Reference reactions contained only gallic acid and H₂O₂ (GA+H₂O₂). Glc is glucose, and number after Glc refers to number of sugar units in the molecule (no number is one)

AldA aldonic acid in reducing end, *diolC4* diol in C4 carbon of the non-reducing end, *KetoneC4* ketone at C4 carbon in the non-reducing end

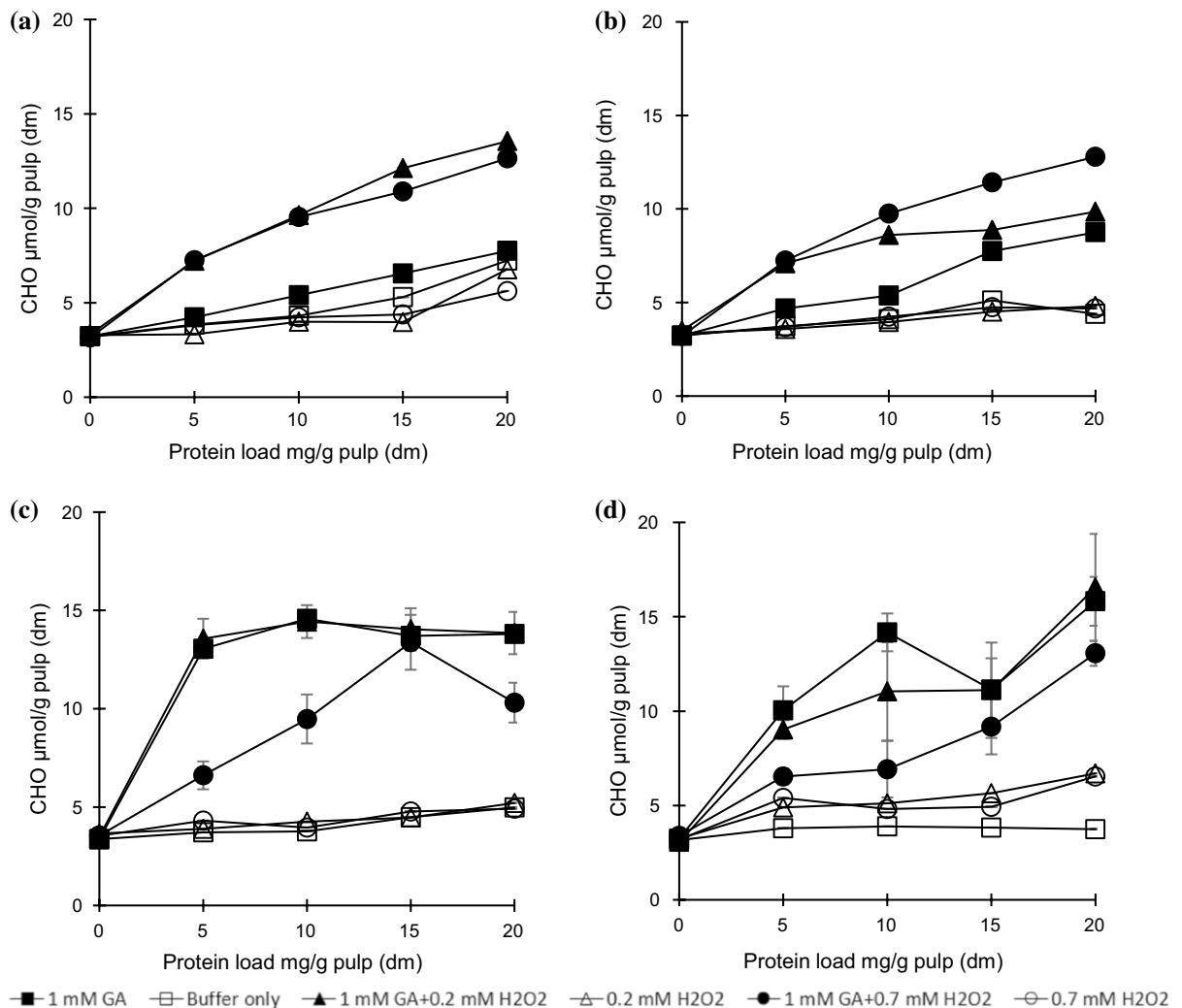


Fig. 1 Concentration of aldehydes [CHO $\mu\text{mol/g}$ cellulose (dm)] in cotton linters after treatment with different dosages of *Tr* AA9A [0–20 mg protein/g substrate (dm)] alone (open squares) and in presence of 1 mM gallic acid (GA, solid squares), 1 mM GA and 0.2 mM H₂O₂ (solid triangles), 1 mM

GA and 0.7 mM H₂O₂ (solid circles), 0.2 mM H₂O₂ (open triangles) or 0.7 mM H₂O₂ (open circles). The treatments were carried out at 45 °C for 6 h at pH 5 (a), pH 6 (b), pH 7 (c) and pH 8 (d). The aldehyde amounts in pulps were determined with the miniaturized TTC assay in 2 ml tubes

enzyme was better, and the reaction was not restricted by H₂O₂ availability. On the contrary, increasing the H₂O₂ concentration to 0.7 mM clearly reduced the enzymatic aldehyde formation. When reaction pH was further increased to eight, even the lower H₂O₂ dosage (0.2 mM) reduced the aldehyde levels (Fig. 1d). Overall, in the test setup the optimum condition for enzymatic oxidation of cotton linters was achieved at pH 7, 45 °C and using the *Tr* AA9A dosage of 5 mg/g pulp (dm) in the presence of 1 mM GA (Fig. 1c). A very similar result was achieved by

supplying the *Tr* AA9A both 1 mM GA and 0.2 mM H₂O₂ (Fig. 1c).

The effect of pH and H₂O₂ concentration to the *Tr* AA9A catalyzed oxidation of the cotton fibres can be due to enzyme (protein) properties and/or non-enzymatic redox chemistry. Reaction pH and H₂O₂ supply has been earlier reported to affect the oxidative activity of the LPMO9B from *Gloeophyllum trabeum*, in reductant dependent manner (Hegnar et al. 2019). The pK_a of the carboxylic acid of GA is 4.0, while the pK_a:s of the phenolic hydroxyls are 8.7,

11.4, and > 13 (Eslami et al. 2010; Pant et al. 2019). In the experimental conditions used in our study (pH 5–8) the carboxylic acid is deprotonated, which promotes electron donation to Cu(II), a requirement for the catalysis. At pH 7–8, the deprotonated GA is also prone to air-oxidation, which leads to formation of H₂O₂ (Strlič et al. 2002; Eslami et al. 2010; Nakamura et al. 2012). This could have diminished the effect of added H₂O₂ into the reaction, as also seen in (Fig. 1a, b). At pH 5–6, the auto-oxidation of GA is expected to be slow (Strlič et al. 2002) and an addition of the H₂O₂ clearly improved the *Tr* AA9A catalyzed oxidation of the cotton linters. In a recent study of Stepnov et al. (2021), it was shown that GA is less susceptible to H₂O₂ producing side-reactions at pH 6 than ascorbic acid, which is commonly used as reductant in LPMO reactions. When LPMO enzymes are not bound to the substrate, they can also catalyze oxidation of reductants (e.g. GA) which again leads to H₂O₂ formation, which can promote the reaction at lower pHs (Kittl et al. 2012; Caldararu et al. 2019). The non-bound LPMOs are however prone to self-oxidation and inactivation, and even protein degradation by H₂O₂ i.e. other means for H₂O₂ provision would be preferred (Bissaro et al. 2017, Paradisi et al. 2019, Filandr et al. 2020). Importantly, as an antioxidant, the GA can also scavenge excess of the hydrogen peroxide and thus protect the LPMO from inactivation (Hegnar et al. 2019). The reported H₂O₂

concentration supporting LPMO activity are in sub-millimolar level (e.g. < 0.2 mM, Bissaro et al. 2017), and as such the, 1 mM GA in the reaction was most likely also protecting the enzyme by inactivation. The transition from the dominance of the antioxidant to pro-oxidant behavior of the GA occurs in ca. neutral pH environment. The negligible or negative effects of hydrogen peroxide addition observed at pH 7 and 8 (Fig. 1c, d), can arise from inactivation of the LPMO by excess H₂O₂ (Bissaro et al. 2017).

Soluble sugars released in the treatment of cotton linters with *Tr* AA9A were analyzed with a UHPLC-IM-MS, using a method combined from Westereng et al. (2016) and Fanuel et al. (2017), in order to verify the enzyme regioselectivity and observed effects of pH and H₂O₂ using an alternative method. The C4 oxidation products are not stable in the highly alkaline solvents commonly used in high resolution HPLC-based carbohydrate analysis. In the improved LC method described by Westereng et al. (2016) the chromatographic separation was done at pH 8 in order to protect the C4 oxidation products. Ion mobility (IM) method introduced by Fanuel et al. (2017) was used to further analyse the C4 oxidized and non-oxidized oligosaccharides (Fig. 2, Table 1). The quantification of the oligosaccharides with the mass spectrometry can be considered semi-quantitative, since the detector responses were converted to sugar concentrations using non-oxidized oligosaccharides as standards.

The samples analyzed with UHPLC-IM-MS originated from the enzymatic treatments [enzyme load 10 mg/g substrate (dm)] of cotton linters carried out at pH 6 or pH 7, 45 °C, in presence of 1 mM GA only or with 1 mM GA and 0.2 mM H₂O₂. In accordance to the earlier results, both C1 and C4 oxidation products were detected, the C4 oxidation products being clearly dominant, according to the relative quantitation using non-oxidized oligosaccharides as standards (Table 1). The lengths of the oxidized oligosaccharides were 2–4 glucose units. Oligosaccharides with ≥ 5 glucose units may have been formed in the enzymatic treatment, but these could not be analysed with the used method. Non-oxidized oligosaccharides were also observed, possibly originating from consequent C1 and C4 oxidations and/or degradation of the oxidized oligosaccharides (Westereng et al. 2016). No soluble sugars were seen in the control reactions, i.e. after treatment with *Tr* AA9A in the absence of GA

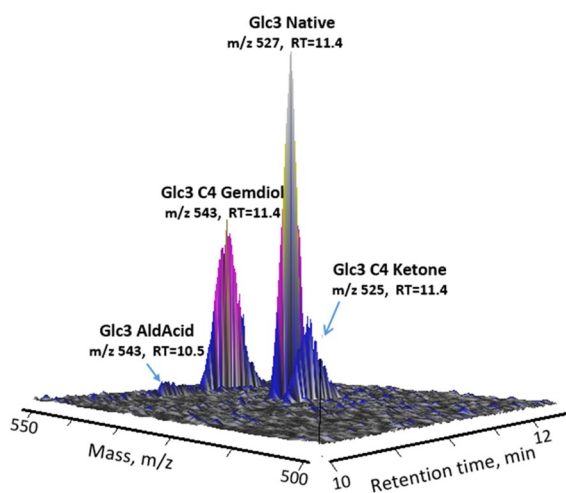


Fig. 2 Separation of cellotriose and its C1 oxidized forms (aldonic acid, AldAcid) and C4 oxidized forms (ketone, gemdiol) using UHPLC-MS

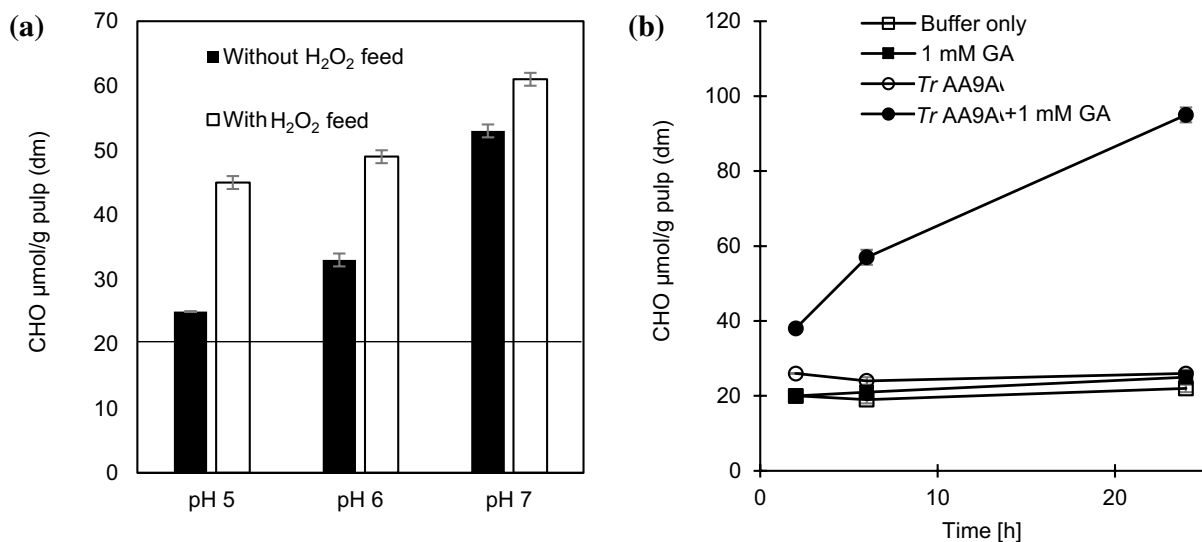


Fig. 3 Effect of pH, H₂O₂ and reaction time on accumulation of aldehydes to softwood kraft pulp in *Tr* AA9A treatment. **a** Concentration of aldehydes [CHO µmol/g cellulose (dm)] in softwood kraft fibres after treatment with *Tr* AA9A [5 mg protein/g substrate (dm)] in presence of gallic acid (GA), or GA and H₂O₂, at pH 5, 6 or 7. The H₂O₂ was added gradually (0.2 mM addition in the beginning and after 2 and 4 h),

reaching in 6 h reaction time accumulative concentration of 0.6 mM. The aldehyde level in non-treated pulp is marked with a horizontal line. **b** Concentration of aldehydes [CHO µmol/g cellulose (dm)] in softwood kraft fibres after treatment with *Tr* AA9A [5 mg protein/g substrate (dm)] in presence of GA for 2, 6 or 24 h at pH 7. The aldehydes were measured in all cases (**a** and **b**) using the TTC assay

or in a reaction lacking the enzyme, confirming that the detected soluble sugar products arose from the LPMO catalyzed reaction. In accordance to the pulp aldehyde analysis, the *Tr* AA9A treatment released more soluble sugars at pH 7 than at pH 6 (Table 1). Addition of 0.2 mM H₂O₂ increased the amount of soluble products, especially when reactions were carried out at pH 6 (Table 1).

Oxidative modification of bleached softwood kraft fibres by *Tr* AA9A: reaction parameters, molecular effects and fibre dissolution kinetics

The *Tr* AA9A was studied in treatment of softwood kraft fibres at pH 5, 6 and 7 using 1 mM GA as reductant in order to verify the effects of the reaction conditions with a technical substrate (Fig. 3a). The enzyme dosage was 5 mg/g substrate (dm) and in part of the reactions H₂O₂ was added in a sequential manner, 0.2 mM per two hours during the 6 h reaction time in order to reduce possible enzyme inactivation by an excess H₂O₂ concentration in the beginning of the experiment. The reaction pH and

H₂O₂ supply affected *Tr* AA9A catalyzed oxidation of softwood kraft fibres in a similar manner as with the cotton linters as substrate: the amount of aldehydes formed in a 6 h treatment was clearly highest, when the reaction was carried out at pH 7, and an addition of H₂O₂ improved the oxidation efficiency essentially at the lower pHs (pH 5 and pH 6) (Fig. 3a). If all of the H₂O₂ would have been stoichiometrically consumed in catalytic fibre cleavages at C4 carbon leading to aldehyde formation, the aldehyde concentration would have been 600 µmol/30 g dry fibres, i.e. 20 µmol/g dry fibres. The treatment of pulp with *Tr* AA9A and 1 mM GA at pH 5 and 6 increased the amount of aldehydes ca 3 and 11 µmol/g pulp, respectively, while with H₂O₂ the values were ca 23 and 27 µmol/g pulp. The added H₂O₂ amount thus corresponds with the increase in aldehydes at pH 5 and 6. At pH 7 the increase in aldehydes was 31 µmol/g pulp with GA only and 39 µmol/g pulp when H₂O₂ was added, suggesting that either the system was not limited by the addition of H₂O₂ and/or enzyme inactivation was hampering the reaction efficiency.

Comparison of *Tr* AA9A LPMO and *Tr* Cel45A endoglucanase in treatment of softwood fibres (at pH

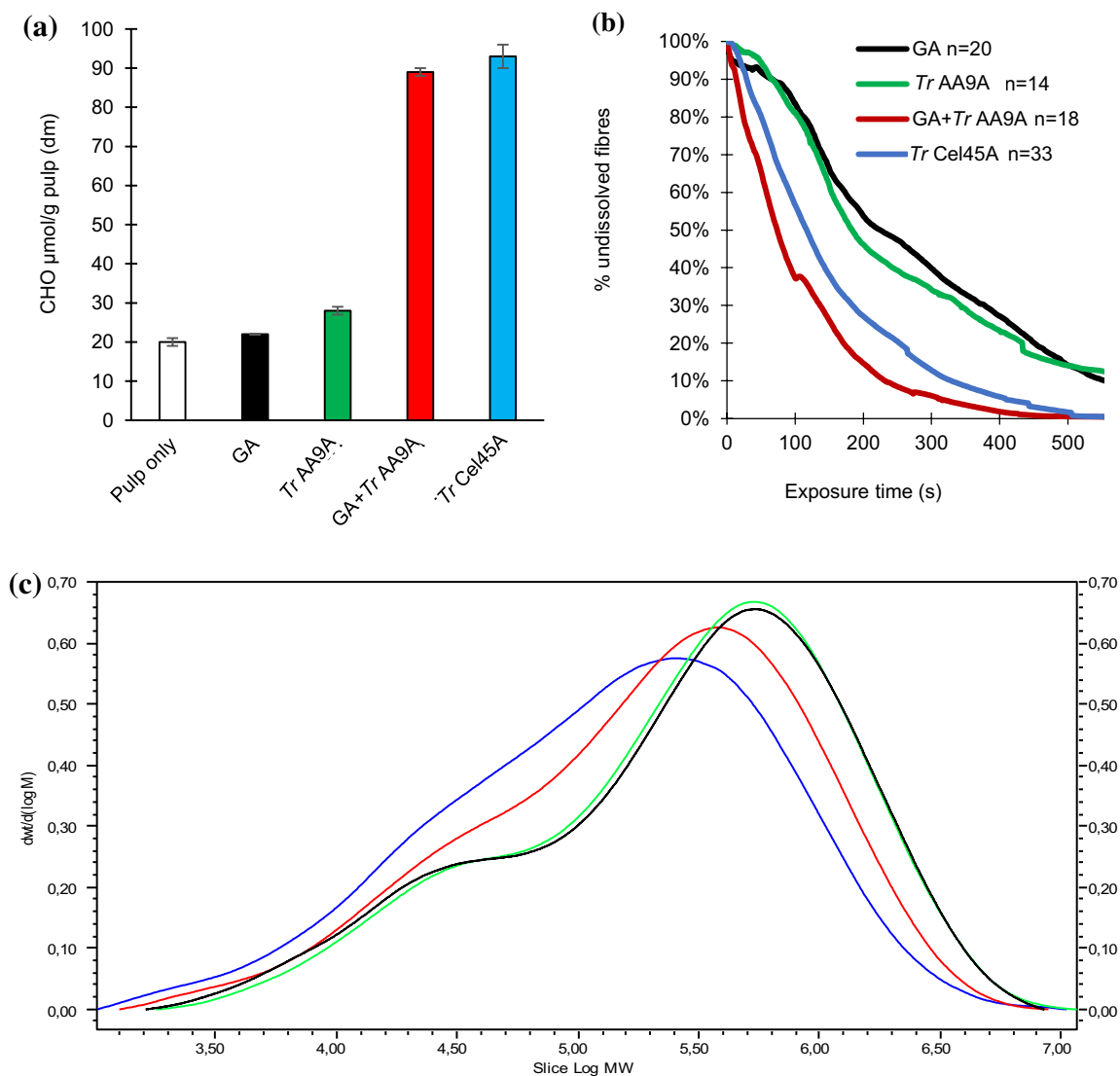


Fig. 4 Comparison of properties of *Tr* AA9A LPMO and *Tr* Cel45A endoglucanase treated softwood kraft fibres. **a** Amount of aldehydes in fibres (measured with TTC assay), **b** Average fibre dissolution rates in CED, analyzed with the microscopy method (n = number of fibres followed) **c** Molar mass distribu-

tions (analyzed with SEC). Color codes: *Tr* AA9A with 1 mM GA (red) and *Tr* Cel45A (blue). Controls were treated with GA only (black) or with *Tr* AA9A without GA (green). The enzyme load was 5 mg/g pulp (dm), and the reactions were carried out at pH 7, 45 °C for 24 h. (Color figure online)

7, 45 °C, enzyme dosage 5 mg/g pulp) are shown in Fig. 4. In contrast to results presented recently by Ceccherini et al. (2021), the LPMO treatment produced similar amount of aldehydes (89 $\mu\text{mol/g pulp}$) in pulp as the endoglucanase treatment (93 $\mu\text{mol/g pulp}$), presumably due to longer treatment time applied here (Fig. 4a). In accordance to Ceccherini et al.

(2021), the cellulose molar mass average of the *Tr* AA9A treated fibers remained high ($M_w = 510$ kDa) compared to the endoglucanase treated fibres ($M_w = 360$ kDa) (Fig. 4c). Small decrease in cellulose molar mass has also been seen by Villares et al. (2017) when using a very high (20 mg/g) *Podospora anserina* LPMO9H enzyme load in a treatment of the

softwood kraft fibres. The clear reduction of cellulose molar mass average is instead typical for endoglucanase treatments, due to hydrolytic cleavage of internal linkages of the cellulose polymers (Grönqvist et al. 2014; Rahikainen et al. 2019).

Dissolution mechanism of the LPMO treated softwood kraft fibres was studied at a single fibre level using a previously published microscopy-based method (Mäkelä et al. 2018; Rahikainen et al. 2019). In this method, the fibres are exposed to CED, an alkaline cellulose solvent, under the microscope, and the dissolution of fibres to the solvent is followed by taking photographs every second upon the exposure. The quantitative rate of fibre dissolution is achieved by calculating the change in visible fibre area in every time point.

First, the LPMO *Tr* AA9A and endoglucanase *Tr* Cel45A treated fibres were compared. Prior dissolution, the light microscopy analysis showed that the morphology of LPMO treated fibres was very similar to non-treated fibres (SI Fig. 2). The results resemble the results of Villares et al. (2017) obtained in a treatment of softwood fibres with *Pa* LPMO9H. The endoglucanase treatment, instead caused cutting of the fibres (SI Fig. 2). When the fibres were analyzed

by the microscopy based method following dissolution of a single fibre to CED, both the *Tr* AA9A (+GA) and *Tr* Cel45A treated fibres exhibited clearly faster dissolution, than the controls treated with GA only (Fig. 4b, SI Video 1). The dissolution curves of *Tr* AA9A and *Tr* Cel45A treated fibres were similar to each other, indicating that despite the morphological differences between the fibres observed in light microscopy the modifications were in both cases sufficient to promote the fibre disintegration in CED (Fig. 4b).

The effect of LPMO treatment on dissolution behavior was further studied by using different enzyme dosages (0.25–2 mg/g pulp) in the treatment (pH 7, 24 h, 1 mM GA as reductant/source of H₂O₂). The amount of aldehydes in the LPMO treated fibres were analyzed by TTC assays to compare the levels of fibre modification (Fig. 5a). The aldehyde amount in pulp increased nearly linearly by increasing the enzyme dosage up to 1 mg/g pulp, after which the doze response ceased, suggesting that enzyme dose was no more limiting the product formation. The CED dissolution curves obtained from treated fibres are shown in Fig. 5b. In the image analysis, it was observed that remnants of some of the fibres

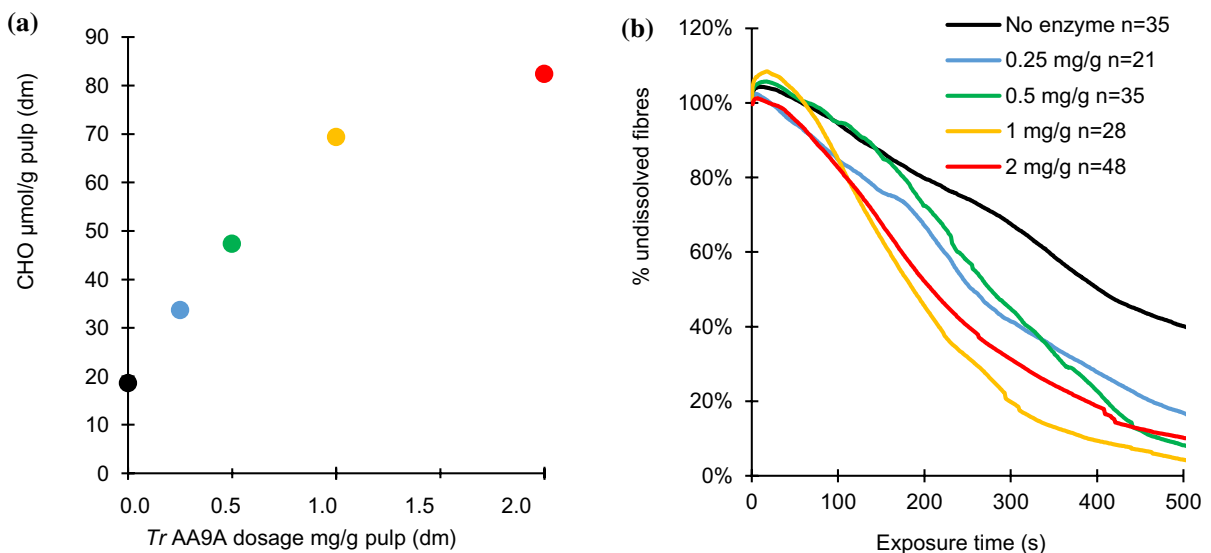


Fig. 5 Dose response of *Tr* AA9A treatment of softwood kraft fibres on **a** Aldehyde accumulation, measured with TTC assay (CHO $\mu\text{mol/g pulp}$) **b** Average fibre dissolution rate to CED of softwood kraft fibres measured with the microscopy method. Color codes: Black=control (no enzyme), Blue 0.2 mg *Tr*

AA9A/g pulp (dm); Green=0.5 mg *Tr* AA9A/g pulp (dm); Orange=1 mg *Tr* AA9A/g pulp (dm); Red=2 mg *Tr* AA9A/g pulp (dm). Control reactions (no enzyme) were carried out with GA only. The reactions were carried out at pH 7, 45 °C for 24 h. (Color figure online)

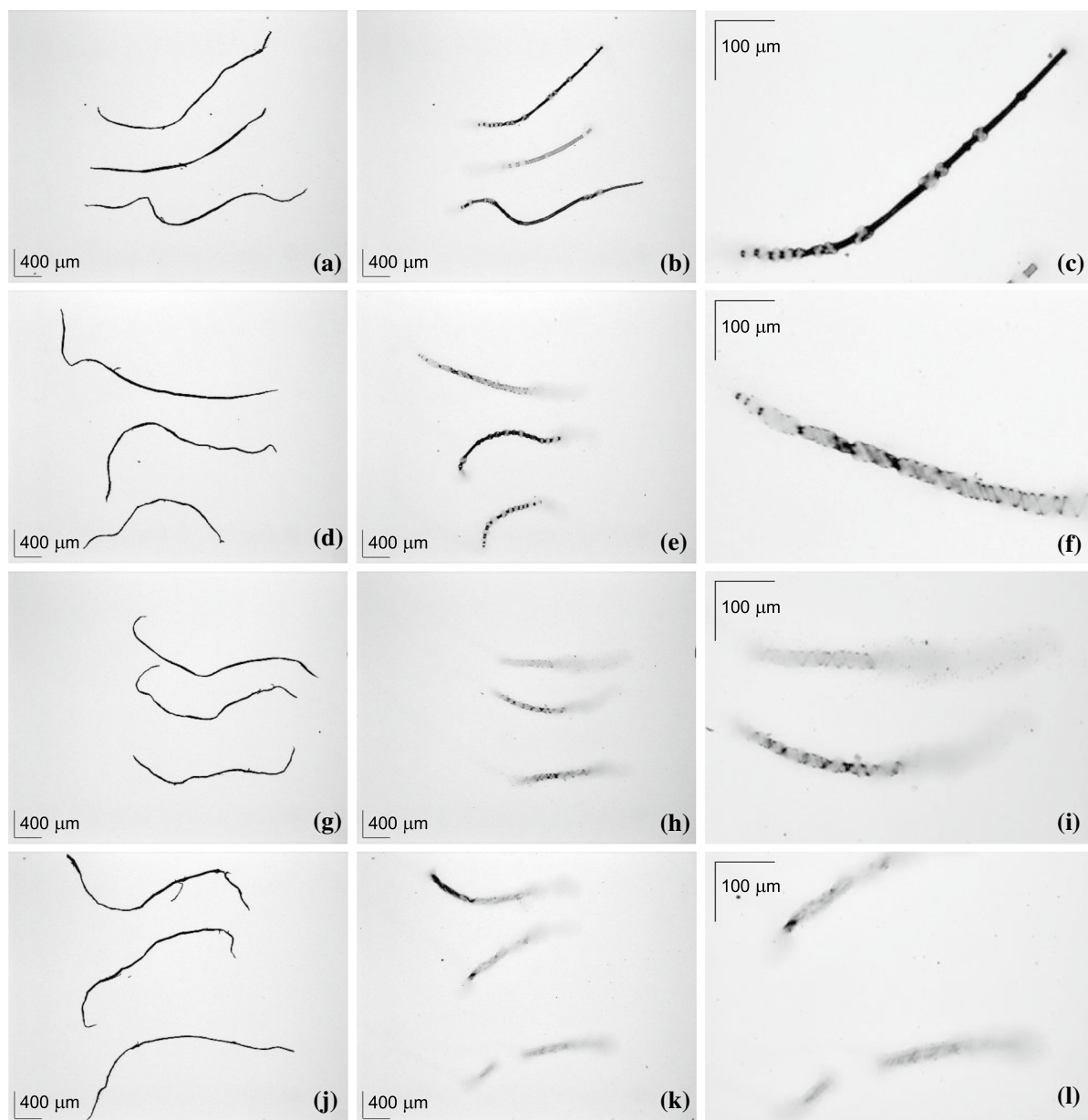


Fig. 6 Microscopic images of softwood kraft fibres treated with GA only (a–c) or with *Tr* AA9A using enzyme dosage of 0.25 mg/g pulp (d–f), 1 mg/g pulp (g–i) and 2 mg/g pulp (j–l) at pH 7, 45 °C and 24 h, at time point 1 s (a, d, g, j) and 150 s

(b, e, h, k) during exposure to CED. The figure c, f, i, j and l are close up views to the individual fibres in b, e, h and k, respectively

(up to 9 fibres/sample) formed under microscope as dark shadows, perhaps composed of small fibre particles. These were in particular observed in samples treated with 0.25–1 mg LPMO (SI Fig. 3). The data from such fibres was removed from the final data set, since the image analysis method interpreted them as

very large fibres. Their formation may however be related to modified fibre structures, which disintegrate upon exposure to CED but do not fully dissolve. The average dissolution rate of *Tr* AA9A treated fibers was faster than the reference, even when the lowest enzyme dosage (0.25 mg/g pulp) was used.

Interestingly, the dissolution was clearly enhanced in samples with relatively low level of oxidative modification (Fig. 5b).

Analysis of the light microscopy images taken during the dissolution, after 150 s of exposure, revealed that the *Tr* AA9A treatment affected dissolution pattern of the fibres in an enzyme dosage dependent manner (Fig. 6). The non-treated fibres exhibited the ballooning-type of swelling, typical for native softwood kraft fibres (Budtova and Navard 2016; Mäkelä et al. 2018) (Fig. 6b, c). This pattern is expected to be caused by restriction of the fibre swelling by the outer cell wall layers (P and S1 layer) (Budtova and Navard 2016; Mäkelä et al. 2018). In fibres treated with lower dosages of *Tr* AA9A (e.g. 0.25–0.5 mg/g), the ballooning effect was observed, in addition also helical structures were frequently seen upon fibre dissolution (Fig. 6d, e). The helical structures are thought to be remnants of degraded outer layers (Budtova and Navard 2016). At higher LPMO dosages (1–5 mg/g pulp), the ballooning effect was strongly reduced, more homogenous dissolution of the fibers was observed (Fig. 6g, h). The homogenous dissolution is also typical for endoglucanase pretreated fibres (Mäkelä et al. 2018). The results suggest that the origin of faster dissolution of the *Tr* AA9A treated fibres would be related to the degradation of the fibre surface structures, limiting the swelling of the fibres.

Conclusion

More sustainable alternatives utilizing biocatalysts instead of harmful chemicals are needed for cellulose dissolution e.g. for textile applications to produce regenerated cellulosic fibres. The role of endoglucanases in this type of applications has been established and commercially used. Here, the enzymatic oxidation of cellulosic fibres to aid the dissolution was studied in more details with *Tr* AA9A LPMO, using GA as an electron donor (reductant). *Tr* AA9A is a 2-domain enzyme, which can oxidize the glucose ring in cellulose chains both at the C4 and C1 position, the C4 position being the preferred mode. Beyond the current work, solely C1 oxidizing LPMOs would be prominent catalysts in improving the fibre reactivity, due to their potential in fibre carboxylation, which in turn could further enhance the cellulose solubility. Our results show that when the phenolic

compound GA is used as reductant in the reaction, the *Tr* AA9A produces the highest fibre oxidation levels at pH 7. The fibre oxidation at acidic pHs (pH 5 and 6) could be clearly improved by addition of H₂O₂, while at neutral and alkaline pH (pH 7 and 8) addition of H₂O₂ had negligible or negative effect on fibre oxidation levels. Optimization the feeding rate for H₂O₂ could protect the LPMOs from inactivation by excess H₂O₂ and thus enable even higher oxidation levels. The oxidative treatment of softwood kraft fibres with *Tr* AA9A facilitated the fibre dissolution rate in CED, which was related to degradation of fibre surface structures that restrict the swelling, while maintaining the cellulose molar mass average relatively high. This type of enzymatically oxidized fibers could provide interesting properties e.g. for regenerated textile fibres.

Author contributions KM, JR, AK and KK: Contributed to the design and conception of the study, and supervision of the work. KM, JR and MK: Contributed to planning, supervision and execution of the circular dichroism experiments, LPMO treatments and TTC assays, NM and HN: measured the soluble oxidation products, NA: contributed to the heterologous production of the enzymes, AM: analyzed the cellulose molecular weights, UH-M: supervised the microscopy analyses and MM: carried out the computational image analysis.

Funding Open Access funding provided by Technical Research Centre of Finland (VTT). The work was funded by CLIC Innovation Ltd New Fibre products project (TEKES Grant No. 3949/31/2015) and the Academy of Finland's Flagship Programme under Projects Nos. 318890 and 318891 (Competence Center for Materials Bioeconomy, FinnCERES). We acknowledge also the support from Project FunEnzFibres, which is funded under the umbrella of ERA-NET Cofund ForestValue by Academy of Finland (Grant No. 326359). ForestValue has received funding from the European Union's Horizon 2020 research and innovation programme under Grant agreement No. 773324. We thank Dr Pedro Loureiro (Novozymes) for valuable advices and Riitta Isoniemi, Mariitta Svanberg and Kirsi Kiiveri (VTT) for technical assistance.

Declarations

Conflict of interest The authors Kaisa Marjamaa, Jenni Rahikainen, Nina Aro and Kristiina Kruus are inventors in patent application WO2019243673—'Improved fibre dissolution with enzymatic treatment' assigned to VTT Technical Research Centre of Finland Ltd. The authors Marika Karjalainen, Natalia Maiorova, Ulla Holopainen-Mantila, Matthieu Molinier, Heli Nygren, Atte Mikkelsen and Anu Koivula have no competing interests.

Open Access This article is licensed under a Creative Commons Attribution 4.0 International License, which permits

use, sharing, adaptation, distribution and reproduction in any medium or format, as long as you give appropriate credit to the original author(s) and the source, provide a link to the Creative Commons licence, and indicate if changes were made. The images or other third party material in this article are included in the article's Creative Commons licence, unless indicated otherwise in a credit line to the material. If material is not included in the article's Creative Commons licence and your intended use is not permitted by statutory regulation or exceeds the permitted use, you will need to obtain permission directly from the copyright holder. To view a copy of this licence, visit <http://creativecommons.org/licenses/by/4.0/>.

References

- Berthold F, Gustafsson K, Sjöholm E, Lindström M (2001) An improved method for the determination of softwood kraft pulp molecular mass distributions. In 11th International symposium on wood and pulping chemistry. pp 363–366
- Bissaro B, Røhr ÅK, Müller G, Chylenski P, Skaugen M, Forsberg Z, Horn SJ, Vaaje-Kolstad G, Eijsink VGH (2017) Oxidative cleavage of polysaccharides by monocopper enzymes depends on H₂O₂. *Nat Chem Biol* 13:1123–1128. <https://doi.org/10.1038/nchembio.2470>
- Boer H, Koivula A (2003) The relationship between thermal stability and pH optimum studied with wild-type and mutant *Trichoderma reesei* cellobiohydrolase Cel7A. *Eur J Biochem* 270:841–848. <https://doi.org/10.1046/j.1432-1033.2003.03431.x>
- Budtova T, Navard P (2016) Cellulose in NaOH–water based solvents: a review. *Cellulose* 23:5–55. <https://doi.org/10.1007/s10570-015-0779-8>
- Caldararu O, Oksanen E, Ryde U, Hedegård ED (2019) Mechanism of hydrogen peroxide formation by lytic polysaccharide monoxygenase. *Chem Sci* 10:576–586. <https://doi.org/10.1039/c8sc03980a>
- Calderaro F, Keser M, Akeroyd M, Bevers LE, Eijsink VGH, Várnai A, van den Berg MA (2020) Characterization of an AA9 LPMO from *Thielavia australiensis*, TausLPMO9B, under industrially relevant lignocellulose saccharification conditions. *Biotechnol Biofuels* 13:195. <https://doi.org/10.1186/s13068-020-01836-3>
- Cannella D, Möllers KB, Frigaard N-U, Jensen PE, Bjerrum MJ, Johansen KS, Felby C (2016) Light-driven oxidation of polysaccharides by photosynthetic pigments and a metalloenzyme. *Nat Comm* 7:1–8. <https://doi.org/10.1038/ncomms11134>
- Ceccherini S, Rahikainen J, Marjamaa K, Sawada D, Grönqvist S, Maloney T (2021) Activation of softwood Kraft pulp at high solids content by endoglucanase and lytic polysaccharide monoxygenase. *Ind Crops Prod* 166:113463. <https://doi.org/10.1016/j.indcrop.2021.113463>
- Coseri S, Biliuta G, Simionescu BC, Stana-Kleinschek K, Ribitsch V, Harabagiu V (2013) Oxidized cellulose—survey of the most recent achievements. *Carbohydr Polym* 93:207–215. <https://doi.org/10.1016/j.carbpol.2012.03.086>
- Eslami AC, Pasanphan W, Wagner BA, Buettner GR (2010) Free radicals produced by the oxidation of gallic acid: an electron paramagnetic resonance study. *Chem Cent J* 4:15. <https://doi.org/10.1186/1752-153X-4-15>
- Fanuel M, Garajova S, Ropartz D, McGregor N, Brumer H, Rogniaux H, Berrin JG (2017) The *Podospira anserina* lytic polysaccharide monoxygenase PaLPMO9H catalyzes oxidative cleavage of diverse plant cell wall matrix glycans. *Biotechnol Biofuels* 10:1–10. <https://doi.org/10.1186/s13068-017-0749-5>
- Filandr F, Kavan D, Kracher D, Laurent CVFP, Ludwig R, Man P, Halada P (2020) Structural dynamics of lytic polysaccharide monoxygenase during catalysis. *Biomolecules* 10:242. <https://doi.org/10.3390/biom10020242>
- Frandsen KEH, Simmons TJ, Dupree P, Poulsen J-CN, Hems-worth GR, Ciano L, Johnston EM, Tovborg M, Johansen KS, von Freiesleben P, Marmuse L, Fort S, Cottaz S, Dri-guez H, Henrissat B, Lenfant N, Tuna F, Baldansuren A, Davies GJ, Lo Leggio L, Walton PH (2016) The molecular basis of polysaccharide cleavage by lytic polysaccharide monoxygenases. *Nat Chem Biol* 12:298–303. <https://doi.org/10.1038/nchembio.2029>
- Grönqvist S, Hakala TK, Kamppuri T, Liittä T, Vehviläinen M, Maloney T, Suurnäkki A (2014) Fibre porosity development of dissolving pulp during mechanical and enzymatic processing. *Cellulose* 21:3667–3676. <https://doi.org/10.1007/s10570-014-0352-x>
- Hansson H, Karkehabadi S, Mikkelsen N, Douglas NR, Kim S, Lam A, Kaper T, Kelemen B, Meier KK, Jones SM, Solomon EI, Sandgren M (2017) High-resolution structure of a lytic polysaccharide monoxygenase from *Hypocrea jecorina* reveals a predicted linker as an integral part of the catalytic domain. *J Biol Chem* 292:19099–19109. <https://doi.org/10.1074/jbc.M117.799767>
- Hegnar O, Petrovic D, Bissaro B, Várnai A, Eijsink V (2019) pH-dependent relationship between catalytic activity and hydrogen peroxide production shown via characterization of a lytic polysaccharide monoxygenase from *Gloeophyllum trabeum*. *Appl Environ Microbiol* 85:1–15. <https://doi.org/10.1128/AEM.02612-18>
- Hemsworth GR, Johnston EM, Davies GJ, Walton PH (2015) Lytic polysaccharide monoxygenases in biomass conversion. *Trends Biotechnol* 33:747–761. <https://doi.org/10.1016/j.tibtech.2015.09.006>
- Hu J, Tian D, Renneckar S, Saddler JN (2018) Enzyme mediated nanofibrillation of cellulose by the synergistic actions of an endoglucanase, lytic polysaccharide monoxygenase (LPMO) and xylanase. *Sci Rep* 8:4–11. <https://doi.org/10.1038/s41598-018-21016-6>
- Hüttner S, Várnai A, Petrović DM, Bach CX, Kim Anh DT, Thanh VN, Eijsink VGH, Larsbrink J, Olsson L (2019) Specific xylan activity revealed for AA9 lytic polysaccharide monoxygenases of the thermophilic fungus *Malbranchea cinnamomea* by functional characterization. *Appl Environ Microbiol* 85:e01408-e1419. <https://doi.org/10.1128/AEM.01408-19>
- Ibarra D, Köpcke V, Ek M (2010) Behavior of different mono-component endoglucanases on the accessibility and reactivity of dissolving-grade pulps for viscose process. *Enzyme Microbiol Technol* 47:355–362. <https://doi.org/10.1016/j.enzmitec.2010.07.010>

- Isogai A, Saito T, Fukuzumi H (2011) TEMPO-oxidized cellulose nanofibers. *Nanoscale* 3:71–85. <https://doi.org/10.1039/c0nr00583e>
- Johansson EE, Lind J (2005) Free radical mediated cellulose degradation during high consistency ozonation. *J Wood Chem Technol* 25:171–186. <https://doi.org/10.1080/02773810500191773>
- Jones SM, Transue WJ, Meier KK, Kelemen B, Solomon EI (2020) Kinetic analysis of amino acid radicals formed in H₂O₂-driven CuI LPMO reoxidation implicates dominant homolytic reactivity. *Proc Natl Acad Sci USA* 117:2–8. <https://doi.org/10.1073/pnas.1922499117>
- Kapur JN, Sahoo PK, Wong AKC (1985) A new method for gray-level picture thresholding using the entropy of the histogram. *Comput Vision Graph Image Process* 29:273–285. [https://doi.org/10.1016/0734-189X\(85\)90125-2](https://doi.org/10.1016/0734-189X(85)90125-2)
- Karlsson J, Saloheimo M, Siika-aho M, Tenkanen M, Penttilä M (2001) Homologous expression and characterization of Cel61A (EG IV) of *Trichoderma reesei*. *Eur J Biochem* 268:6498–6507. <https://doi.org/10.1046/j.0014-2956.2001.02605.x>
- Kittl R, Kracher D, Burgstaller D, Haltrich D, Ludwig R (2012) Production of four *Neurospora crassa* lytic polysaccharide monoxygenases in *Pichia pastoris* monitored by a fluorimetric assay. *Biotechnol Biofuels* 5:79. <https://doi.org/10.1186/1754-6834-5-79>
- Kont R, Pihlajaniemi V, Borisova AS, Aro N, Marjamaa K, Loogen J, Büchs J, Eijsink VGH, Kruus K, Våljamäe P (2019) The liquid fraction from hydrothermal pretreatment of wheat straw provides lytic polysaccharide monoxygenases with both electrons and H₂O₂ co-substrate. *Biotechnol Biofuels* 12:235. <https://doi.org/10.1186/s13068-019-1578-5>
- Kont R, Bissaro B, Eijsink VGH, Våljamäe P (2020) Kinetic insights into the peroxygenase activity of cellulose-active lytic polysaccharide monoxygenases (LPMOs). *Nat Comm* 11:5786. <https://doi.org/10.1038/s41467-020-19561-8>
- Kuusik S, Kont R, Kuusik P, Heering A, Sørli M, Bissaro B, Eijsink VGH, Våljamäe P (2019) Kinetic insights into the role of the reductant in H₂O₂-driven degradation of chitin by a bacterial lytic polysaccharide monoxygenase. *J Biol Chem* 294:1516–1528. <https://doi.org/10.1074/jbc.RA118.006196>
- Langston JA, Shaghasi T, Abbate E, Xu F, Vlasenko E, Sweeney MD (2011) Oxidoreductive cellulose depolymerization by the enzymes cellobiose dehydrogenase and glycoside hydrolase 61. *Appl Environ Microbiol* 77:7007–7015. <https://doi.org/10.1128/AEM.05815-11>
- Li H, Legere S, He Z, Zhang H, Li J, Yang B, Zhang S, Zhang L, Zheng L, Ni Y (2018) Methods to increase the reactivity of dissolving pulp in the viscose rayon production process: a review. *Cellulose* 25:3733–3753. <https://doi.org/10.1007/s10570-018-1840-1>
- Lo Leggio L, Simmons TJ, Poulsen JCN, Frandsen KEH, Hemsworth GR, Stringer MA, von Freiesleben P, Tovborg M, Johansen KS, de Maria L, Harris P, Soong CL, Dupree P, Tryfona T, Lenfant N, Henrissat B, Davies GJ, Walton PH (2015) Structure and boosting activity of a starch-degrading lytic polysaccharide monoxygenase. *Nat Comm* 6:5961. <https://doi.org/10.1038/ncomms6961>
- Mäkelä V, Wahlström R, Holopainen-Mantila U, Kilpeläinen I, King AWT (2018) Clustered single cellulosic fiber dissolution kinetics and mechanisms through optical microscopy under limited dissolving conditions. *Biomacromol* 19:1635–1645. <https://doi.org/10.1021/acs.biomac.7b01797>
- Meier KK, Jones SM, Kaper T, Hansson H, Koetsier MJ, Karkehabadi S, Solomon EI, Sandgren M, Kelemen B (2018) Oxygen activation by Cu LPMOs in recalcitrant carbohydrate polysaccharide conversion to monomer sugars. *Chem Rev* 118:2593–2635. <https://doi.org/10.1021/acs.chemrev.7b00421>
- Molinier M, Häme T, Ahola H (2005) in *Image Analysis: 14th Scandinavian Conference, SCIA 2005, Joensuu, Finland, June 19–22, 2005*. Proceedings, eds. H. Kalviainen, J. Parkkinen and A. Kaarna, Springer Berlin Heidelberg, Berlin, Heidelberg, 2005, pp 141–150
- Moreau C, Tapin-Lingua S, Grisel S, Gimbert I, le Gall S, Meyer V, Petit-Conil M, Berrin JG, Cathala B, Villares A (2019) Lytic polysaccharide monoxygenases (LPMOs) facilitate cellulose nanofibrils production. *Biotechnol Biofuels* 12:13–17. <https://doi.org/10.1186/s13068-019-1501-0>
- Müller G, Várnai A, Johansen KS, Eijsink VGH, Horn SJ (2015) Harnessing the potential of LPMO-containing cellulase cocktails poses new demands on processing conditions. *Biotechnol Biofuels* 8:187. <https://doi.org/10.1186/s13068-015-0376-y>
- Nakamura K, Yamada Y, Ikai H, Kanno T, Sasaki K, Niwano Y (2012) Bactericidal action of photoirradiated gallic acid via reactive oxygen species formation. *J Agric Food Chem* 60:10048–10054. <https://doi.org/10.1021/jf303177p>
- Obolenskaya AV, Elnitskaya ZP, Leonovitch AA (1991) Determination of aldehyde groups in oxidized pulps. In *Laboratory Manipulations in Wood and Cellulose Chemistry*, Ecologia, pp 211–212
- Pant AF, Özkasikci D, Fürtauer S, Reinelt M (2019) The effect of deprotonation on the reaction kinetics of an oxygen scavenger based on gallic acid. *Fron Chem* 7:1–7. <https://doi.org/10.3389/fchem.2019.00680>
- Paradisi A et al (2019) Formation of a copper(II)-tyrosyl complex at the active site of lytic polysaccharide monoxygenases following oxidation by H₂O₂. *Am Chem Soc*. <https://doi.org/10.1021/jacs.9b09833>
- Patel I, Ludwig R, Haltrich D, Rosenau T, Potthast A (2011) Studies of the chemoenzymatic modification of cellulose pulps by the laccase-TEMPO system. *Holzforchung* 65:475–481. <https://doi.org/10.1515/HF.2011.035>
- Phillips CM, Beeson WT, Cate JH, Marletta MA (2011) Cellobiose dehydrogenase and a copper-dependent polysaccharide monoxygenase potentiate cellulose degradation by *Neurospora crassa*. *ACS Chem Biol* 6:1399–1406. <https://doi.org/10.1021/cb200351y>
- Pierce BC, Witttrup J, Wichmann J, Meyer AS (2017) Oxidative cleavage and hydrolytic boosting of cellulose in soybean spent flakes by *Trichoderma reesei* Cel61A lytic polysaccharide monoxygenase. *Enzyme Microb Technol* 98:58–66. <https://doi.org/10.1016/j.enzmictec.2016.12.007>

- Potthast A, Rosenau T, Kosma P (2006) Analysis of oxidized functionalities in cellulose. In: Klemm D (ed) Polysaccharides II. Advances in polymer science, vol 205. Springer, Berlin, pp 1–48
- Potthast A, Kostic M, Schiehser S, Kosma P, Rosenau T (2007) Studies on oxidative modifications of cellulose in the periodate system: molecular weight distribution and carbonyl group profiles. *Holzforschung* 61:662–667. <https://doi.org/10.1515/HF.2007.099>
- Quinlan RJ, Sweeney MD, Lo L, Otten H, Poulsen JN, Tryfona T, Walter CP, Dupree P, Xu F, Davies GJ, Walton PH (2011) Insights into the oxidative degradation of cellulose by a copper metalloenzyme that exploits biomass components. *PNAS* 108:15079–15084. <https://doi.org/10.1073/pnas.1105776108>
- Quintana E, Roncero MB, Vidal T, Valls C (2017) Cellulose oxidation by laccase-TEMPO treatments. *Carbohydr Polym* 157:1488–1495. <https://doi.org/10.1016/j.carbpol.2016.11.033>
- Rahikainen J, Ceccherini S, Molinier M, Holopainen-Mantila U, Reza M, Väisänen S, Puranen T, Kruus K, Vuorinen T, Maloney T, Suurnäkki A, Grönqvist S (2019) Effect of cellulase family and structure on modification of wood fibres at high consistency. *Cellulose* 26:5085–5103. <https://doi.org/10.1007/s10570-019-02424-x>
- Rahkamo L, Siika-aho M, Viikari L, Leppanen T, Buchert J (1998) Effect of cellulases and hemicellulases on alkali solubility of dissolving pulps. *Holzforschung* 52:630–634. <https://doi.org/10.1515/hfsg.1998.52.6.630>
- Rodríguez-Zúñiga UF, Cannella D, Giordano RDC, Giordano RDL, Jørgensen H, Felby C (2015) Lignocellulose pretreatment technologies affect the level of enzymatic cellulose oxidation by LPMO. *Green Chem* 17:2896–2903. <https://doi.org/10.1039/c4gc02179g>
- Saloheimo M, Nakari-Setälä T, Tenkanen M, Penttilä M (1997) cDNA cloning of a *Trichoderma reesei* cellulase and demonstration of endoglucanase activity by expression in yeast. *Eur J Biochem* 249:584–591. <https://doi.org/10.1111/j.1432-1033.1997.00584.x>
- Singh RK, Blossom BK, Russo DA, Oort B, Croce R, Jensen PE, Felby C, Bjerrum MJ (2019) Thermal unfolding and refolding of a lytic polysaccharide monooxygenase from *Thermoascus aurantiacus*. *RSC Adv* 9:29734–29742. <https://doi.org/10.1039/C9RA05920B>
- Song B, Li B, Wang X, Shen W, Park S, Collings C, Feng A, Smith SJ, Walton JD, Ding SY (2018) Real-time imaging reveals that lytic polysaccharide monooxygenase promotes cellulase activity by increasing cellulose accessibility. *Biotechnol Biofuels* 11:1–11. <https://doi.org/10.1186/s13068-018-1023-1>
- Stepnov AA, Forsberg Z, Sørli M, Nguyen G-S, Wentzel A, Røhr ÅK, Eijsink VGH (2021) Unraveling the roles of the reductant and free copper ions in LPMO kinetics. *Biotechnol Biofuels* 14:28. <https://doi.org/10.1186/s13068-021-01879-0>
- Strlič M, Radovič T, Kolar J, Pihlar B (2002) Anti- and prooxidative properties of gallic acid in fenton-type systems. *J Agric Food Chem* 50:6313–6317. <https://doi.org/10.1021/jf025636j>
- Tanghe M, Danneels B, Camattari A, Glieder A, Vandenberghe I, Devreese B, Stals I, Desmet T (2015) Recombinant expression of *Trichoderma reesei* Cel61A in *Pichia pastoris*: optimizing yield and N-terminal processing. *Mol Biotechnol* 57:1010–1017. <https://doi.org/10.1007/s12033-015-9887-9>
- Vaaje-Kolstad G, Westereng B, Horn SJ, Liu Z, Zhai H, Sørli M, Eijsink VGH (2010) An oxidative enzyme boosting the enzymatic conversion of recalcitrant polysaccharides. *Science (new York)* 330:219–222. <https://doi.org/10.1126/science.1192231>
- Valls C, Javier Pastor FI, Blanca Roncero M, Vidal T, Diaz P, Martínez J, Sv V (2019) Assessing the enzymatic effects of cellulases and LPMO in improving mechanical fibrillation of cotton linters. *Biotechnol Biofuels* 12:1–14. <https://doi.org/10.1186/s13068-019-1502-z>
- Vandhana TM, Reyre JL, Sushmaa D, Berrin JG, Bissaro B, Madhuprakash J (2022) On the expansion of biological functions of lytic polysaccharide monooxygenases. *New Phytol* 233:2380–2396. <https://doi.org/10.1111/nph.17921>
- Villares A, Moreau C, Bennati-Granier C, Garajova S, Foucat L, Falourd X, Saake B, Berrin J-G, Cathala B (2017) Lytic polysaccharide monooxygenases disrupt the cellulose fibers structure. *Sci Rep* 7:40262. <https://doi.org/10.1038/srep40262>
- Westereng B, Arntzen M, Aachmann F, Várnai A, Eijsink VGH, Wittrup Agger J (2016) Simultaneous analysis of C1 and C4 oxidized oligosaccharides, the products of lytic polysaccharide monooxygenase acting on cellulose. *J Chromatogr A* 1445:46–54. <https://doi.org/10.1016/j.chroma.2016.03.064>

Publisher's Note Springer Nature remains neutral with regard to jurisdictional claims in published maps and institutional affiliations.